Magnetic Resonance and Fluorine-18 Deoxyglucose Imaging in the Investigation of a Spinal Cord Tumor

Guest Editor: Abass Alavi
Case Presentation by Eric Kramer*, and William Wegener†
Discussion by Jane Alavi‡

From the case records of the Hospital of the University of Pennsylvania, Philadelphia, Pennsylvania

J Nucl Med 1990; 31:360–364

CLINICAL HISTORY

A 19-yr-old man was admitted to the hospital for consideration of ablative chemotherapy followed by autologous bone marrow rescue for a cervical spinal core glioblastoma multiforme. He presented to another institution after two weeks of progressive neck stiffness and left arm weakness, where initial magnetic resonance image (MRI) studies showed a markedly enlarged cervical spinal cord which enhanced following i.v. administration of gadolinium DTPA (Fig. 1). A decompressive laminectomy and biopsy were performed. The histopathologic diagnosis was glioblastoma multiforme. Hyperfractionated radiation was given to the involved site to a total dose of 5400 cGy. Six days after completion of irradiation, he came to the Children's Hospital of Philadelphia. An MRI study at that time documented postlaminectomy changes, including hemorrhage. As shown in Figure 2, the cervical spinal cord remained markedly enlarged with a lobulated enhancing mass extending from C2-C6.

There was a history of delayed achievement of motor skills as a child. He was now a college student and had no history of trauma or toxic exposures. There was no family history of brain tumors.

The temperature was 38.9°C, pulse 86, respirations 18, blood pressure 120/76. On physical examination, he was alert and oriented and apprehensive. The general physical examination revealed radiation changes over the skin of the back of the neck and chest. The neurologic examination revealed no cognitive, language, or memory deficits. The cranial nerves were intact. There was atrophy of the left upper extremity and a spastic left hemiparesis that was worse in the arm than the leg. Bulk, tone, and power were normal on the right side. Cerebellar function was normal. He gave inconsistent responses to the sensory examination for all modalities. Deep tendon reflexes were diminished in the left upper extremity, increased in the left lower extremity, and normal on the right side. The Babinski sign was present on the left. Walking was accomplished with the left leg in external rotation and with a slight circumduction at the left hip.

Laboratory examinations were normal. After bilateral iliac marrow harvesting and placement of a Broviac catheter, he received marrow ablative chemotherapy with Thiotepa, VP 16, and BCNU. His marrow was reinfused 72 hr later. His white count fell to 0 on the 9th day after chemotherapy. On day 15, his absolute neutrophil count rose above 500/mm^3. He had severe mucositis, requiring parenteral morphine and hyperalimentation. He was discharged on day 39 post-bone marrow reinfusion.

MRI scanning was performed on days 7, 14, 28, and 64 after transplant. On the first 3 scans, central necrosis within the tumor mass was observed. The MRI study from day 28 again showed a lobulated enhancing mass (Fig. 3). Except for some new posterior extension at the C4-C5 disk space, there was no significant change from earlier images such as shown in Figure 2. On approximately day 48, he began to have recurrent neck pain. The distal left upper extremity weakness, which had begun to resolve, once again became apparent and progressive. A procedure was performed to distinguish whether this clinical deterioration was due to recurrent tumor or radiation necrosis.

Received Dec. 7, 1989; revision accepted Dec. 8, 1989.
For reprints contact: Abass Alavi, MD, Division of Nuclear Medicine, Department of Radiology, Hospital of the University of Pennsylvania, 3400 Spruce St., Philadelphia, PA 19104.
* Clinical Fellow, Neurooncology Section, Children's Hospital of Philadelphia, Philadelphia, PA.
† Staff Physician, Associate Professor of Medicine, Hematology/Oncology Section, Dept. of Medicine, Hospital of the University of Pennsylvania, Philadelphia, PA.
‡ Clinical Fellow, Division of Nuclear Medicine, Dept. of Radiology, Hospital of the University of Pennsylvania, Philadelphia, PA.

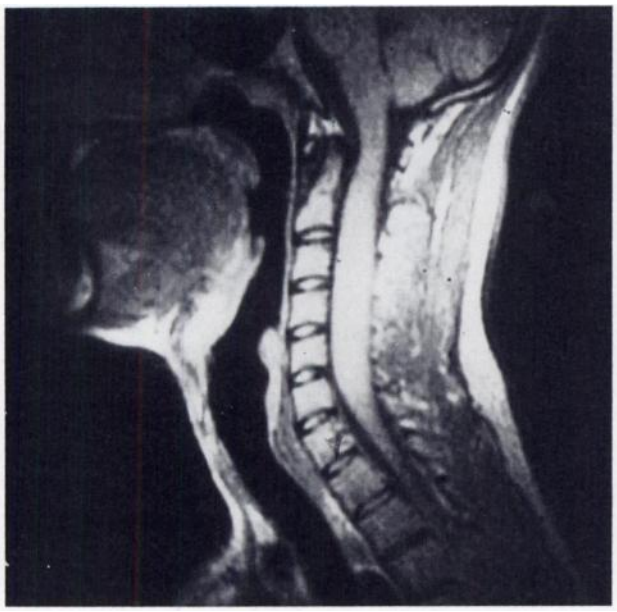

FIGURE 1
Initial MRI study at another institution using a FONAR system (0.3 Tesla) with TR = 600 ms, TE = 30 ms. Sagittal image shows markedly enlarged spinal cord throughout entire cervical region.

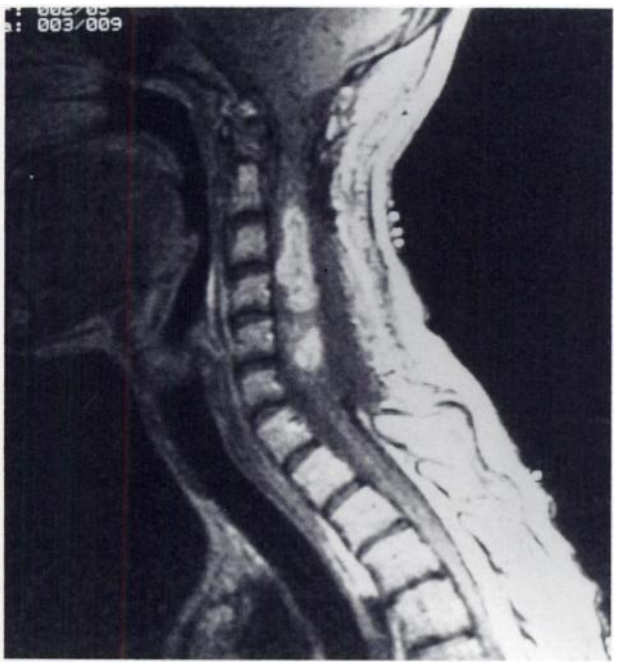

FIGURE 2
Gadolinium DTPA-enhanced T1-weighted sagittal image acquired on a 1.5 Tesla GE system following extensive cervical laminectomy. There is marked enlargement of the cervical spinal cord with the tumor delineated as a lobulated enhancing mass extending from C2-C6. Precontrast images showed hemorrhagic tumor regions at C3-C4.

RADIOGRAPHIC AND NUCLEAR MEDICINE FINDINGS

The patient was referred for a positron emission tomography (PET) study of the cervical spine using ^{18}F-fluorodeoxyglucose (FDG) to examine the metabolic activity of the lesion seen on MRI to differentiate tumor necrosis from active tumor. A 5-mCi dose was administered intravenously, and 40 min later scanning of the upper cervical spine was begun. Images were acquired over 40 min on the PENN PET system, which is based on Anger gamma camera technology, uses a stationary hexagonal array of six positron-sensitive NaI(Th) detectors, and presently allows a spatial resolution of 6–7 mm uniform over all three dimension (*1*). The 10-cm field of view is large enough to image a whole brain and is divided by software into fifty 2-mm axial slices. Transaxial, sagittal, and coronal slices can be viewed following tomographic reconstruction.

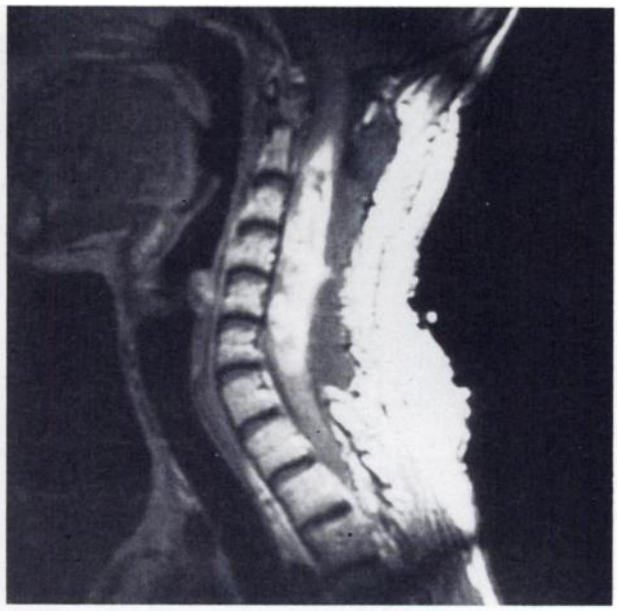

FIGURE 3
Gadolinium DTPA-enhanced T1-weighted sagittal image obtained on a 1.5-Tesla GE system nearly one month after bone marrow transplant. Spinal cord tumor is again seen as lobulated enhancing mass from C2-C7. Some posterior extension is seen at the C4-C5 disk space; otherwise, there are no apparent significant changes from earlier studies.

The midsagittal FDG-PET image in Figure 4 shows markedly increased activity throughout the cervical spinal cord. The region involved corresponds with the region of abnormal involvement seen on previous MRIs (Figs. 1-3). This finding was interpreted as consistent with a diagnosis of tumor recurrence or residual.

In a separate session using 4 mCi of FDG, images of the entire brain also were obtained. As shown in Figure 5, these images are grossly abnormal. Activity appears preserved in the primary sensory motor and visual cortices, the subcortical nuclei, and the cerebellum while there is marked global cortical hypoactivity with all lobes affected in a widespread, symmetric, and nonfocal manner. This pattern of diffuse decreased activity probably represents pronounced cortical functional im-

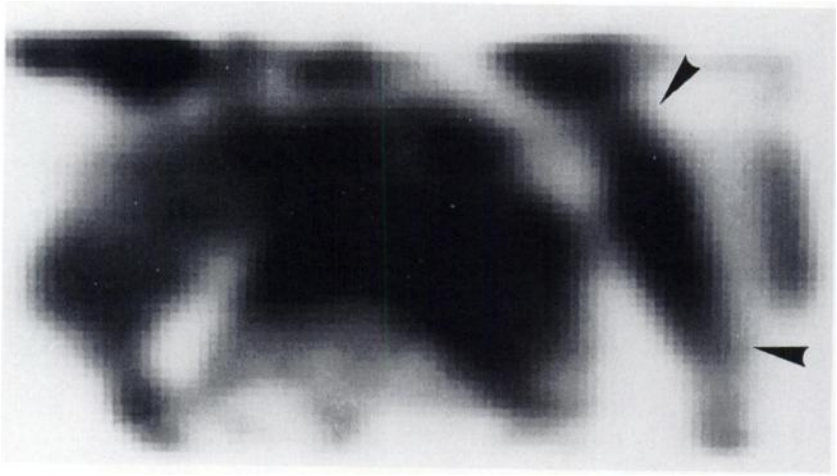

FIGURE 4
PET-FDG midsagittal image of the neck. Arrows delineate region of increased activity which corresponds to the region of cervical spine tumor involvement seen on MRI.

pairment secondary to neuronal disconnections in the cervical spine.

DISCUSSION

This patient was treated aggressively for a malignant spinal cord tumor. Neoplasms of the spinal cord constitute ~15% of all central nervous system tumors. The majority are either Schwannomas (29%), meningiomas (25%), or metastases (23%). Twenty-two percent are glial tumors of astrocytic or ependymal origin. Ependymomas predominate in the filum terminale while astrocytomas are more frequent at higher spinal levels. Primary tumors of the spinal cord behave much like their intracranial counterparts (*2*), i.e., high-grade tumors are extremely malignant with a survival measured in months rather than years, while low-grade tumors can sometimes be cured surgically. Treatment of high-grade lesions remains suboptimal and controversial.

This patient exhibited symptoms of neurologic deterioration 3 mo after treatment. The most likely explanation would be that the tumor was unresponsive to treatment and was extending to involve a larger area of the cord. However, radiation-induced necrosis of the cord could be associated with similar symptoms. In general, radiation injury to the brain and spinal cord does not become clinically manifest for many months or years after treatment is completed, so this seems unlikely in the present case. It is possible, however, that the high-dose chemotherapy could have potentiated the effect of irradiation, resulting in the early appearance of radiation necrosis. The PET scan was performed in order to help differentiate progressive tumor from radiation damage. This technique has been found to be useful in the study of nervous system tumors, especially post-radiation therapy. Brain tumors have been studied in many centers; spinal cord tumors have been described in much smaller numbers. The use of [^{18}F]FDG is based on the observations of Blasberg et al. in an autoradiographic model, that deoxyglucose labeled with ^{14}C was taken up by malignant tumors and retained within the tumors for a prolonged time (*3*). This permits scanning in vivo with measurement of regional metabolic rate for glucose in different areas of the brain. Since malignant cells appear to switch their metabolism to anaerobic glycolysis as the tumor types become more malignant, it was anticipated that the utilization of glucose (and the uptake of deoxyglucose) would be greater for malignant tumors than for benign tumors. This has been borne out in the results of brain tumor PET studies.

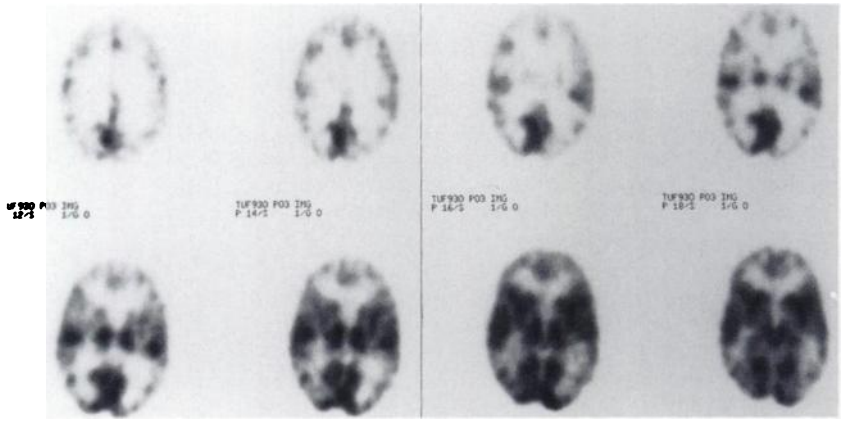

FIGURE 5
PET-FDG select transaxial brain images. There is preservation of activity in the motorsensory strip and visual cortex with marked global hypometabolism in the rest of the cortex. Activity also appears preserved in the subcortical nuclei and cerebellum (not shown here).

It has been found that high-grade astrocytomas (grade III and IV and glioblastomas) are usually associated with high metabolic rate for glucose and that low-grade (grade I and II) usually have a low or normal glucose metabolism. In a report by DiChiro et al. (*4*), a focus of increased activity (hot spot) was seen in all high-grade tumors, but in only 10% of low-grade tumors. In our series, 15 out of 24 high-grade tumor patients had increased glucose metabolic rate in the lesion compared with 1 out of 5 low-grade tumors (*5*). These patients were studied at various time periods after radiation therapy or chemotherapy, so the status of the tumor activity was not always known at the time of the PET scan.

Recently, it has been shown in a group of 12 patients with low-grade astrocytomas that the PET scan revealed a focus of hypermetabolism when the tumors underwent malignant degeneration (*6*). In some cases, prior PET scans showed low metabolism only, so it was inferred that the malignant change was associated with a metabolic change.

The FDG-PET appearance of brain tumors seems to correlate better than CT scans with tumor grade (*7*). Most high-grade neoplasms are enhancing lesions, but the CT scan appearance is not always diagnostic. Some low-grade lesions or necrotic areas enhance, and some high-grade tumors do not enhance.

PET appears to have made a significant contribution to the diagnosis of radiation necrosis. This condition is being seen more commonly in recent years due to more aggressive treatments, such as high-dose interstitial therapy (intratumor implantation of radioactive sources). The CT scans reveal large enhancing areas surrounded by edema, essentially mimicking recurrent tumor. However, the PET scans usually show decreased glucose utilization in these areas, thus distinguishing them from malignant tumor. Patronas et al. (*8*) reported two cases of radiation necrosis, which were diagnosed by PET and confirmed histologically. Subsequently, the same group (*9*) described 10 cases of post-radiation necrosis and 4 cases of post-chemotherapy necrosis (after intracarotid BCNU). There was reduced metabolic activity in all, usually confined to the white matter. A recent report from San Francisco, where interstitial therapy is under investigation, indicated that the PET had 84% accuracy in differentiating tumor recurrence from radiation injury in 34 patients (*10*). These workers used rubidium-82 as a blood brain barrier tracer to localize the lesion and compared glucose metabolic rate in this area to the activity in the adjacent brain. In 17 of 21

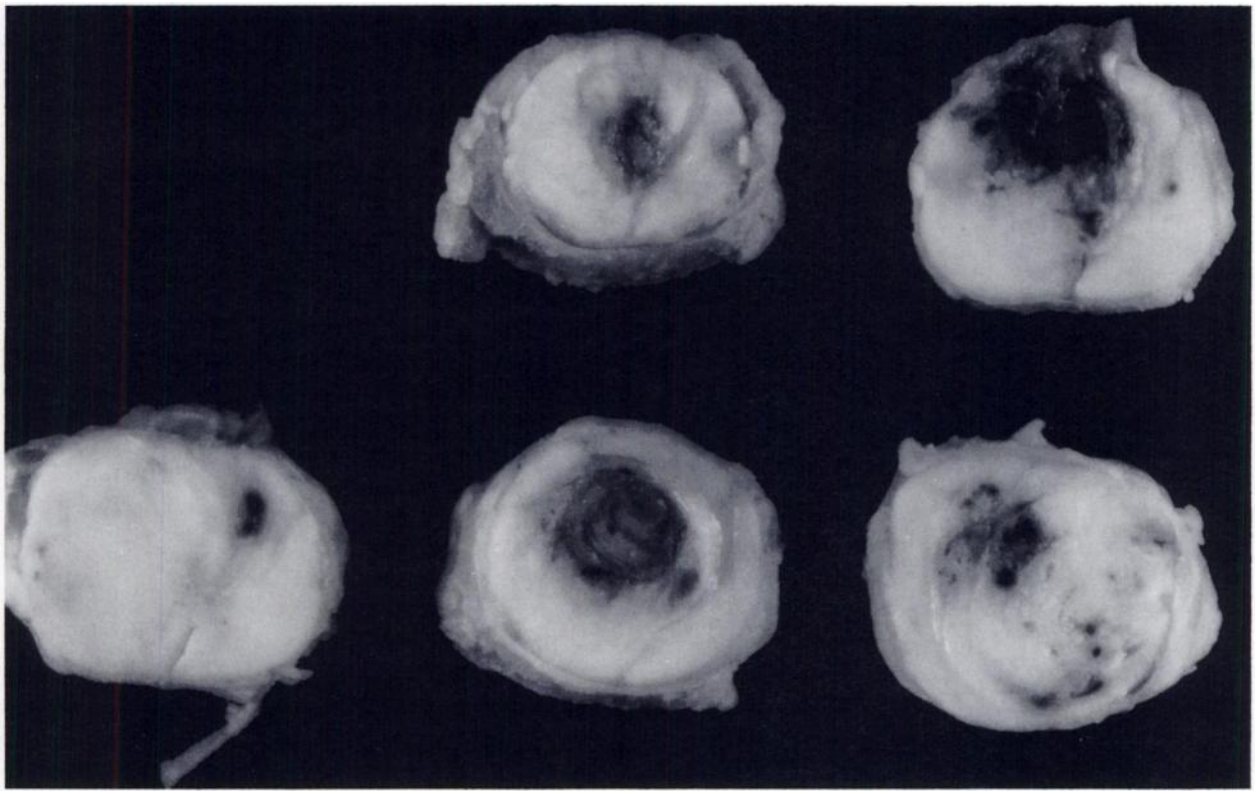

FIGURE 6
Gross pathology specimen obtained at autopsy. Representative transverse sections of cervical-thoracic spinal cord showing extensive distortion of normal anatomy secondary to diffusely infiltrating hemorrhagic, necrotic tumor. The autopsy findings correspond exactly to the abnormalities noted on MRI and PET images.

cases of radiation injury, the PET showed lower glucose metabolism in the lesion, and in 15 of 17 cases of active tumor, the PET showed increased metabolism. Interestingly, careful pathologic examination of these specimens usually revealed some tumor cells in the radiation necrosis cases, but the clinical course was stable for many months, suggesting that the lack of metabolic activity on PET scan correlated with a clinically less aggressive malignancy.

Clinical prognostic studies with PET scans have supported the concept that metabolic rate can predict the clinical course in many patients. It is interesting to speculate that some of the metabolically inactive lesions in our patients with histologically high-grade tumors could have been due to radiation necrosis, since many patients were studied after treatment. In our series, the prognosis did correlate with the metabolic rate. The median survival after PET scan was 7 mo for patients with hypermetabolic lesions and 33 mo for those with low metabolic lesions (*5*). In the study of Patronas et al. (*11*), the survivals were 5 mo versus 19 mo for patients with hypermetabolic versus hypometabolic tumors, respectively. The reasons for these results are probably multiple, but presumably therapy-induced tumor suppression or necrosis accounts for low activity and prolonged survival in some patients.

In other cases, the tumors may be so small that the resolution of PET does not permit a hypermetabolic area to be visualized, and death from tumor occurs much later after growth to a lethal size.

In the case under discussion, the tumor area was clearly quite active metabolically. This indicated that the tumor was growing despite an appearance of therapy-induced necrosis on the MRI scan. There has been little experience with PET with spinal cord malignancies because of the need for high resolution in this small structure. With the development of more advanced PET technology, this has become possible. In one series (*12*) it was found that the glucose utilization of the normal spinal cord was lower than white matter of normal brain. In six patients with tumors of the brain stem or cord, the glucose metabolism was higher than normal in grade III and IV astrocytomas, but lower than normal in low-grade tumors.

The patient under discussion was found to have a high metabolic rate region in the spinal cord which matched the tumor area on MRI scan. Thus, it is most probable that he had persistent malignancy there rather than radiation change.

CLINICAL OUTCOME

This patient continued to deteriorate neurologically over the next several weeks. The MRI of the cervical cord two weeks after the PET scan demonstrated tumor progression. At that time, a decision was made to keep the patient comfortable. He died one month later. Autopsy revealed tumor in the cervical cord extending superiorly into the medulla and inferiorly down into the thoracic spinal cord (Fig. 6). Histologic examination of the tumor confirmed the diagnosis of glioblastoma multiforme.

ACKNOWLEDGMENTS

This material was presented and discussed at the Philadelphia Nuclear Medicine Conference, December 1989.

Supported by Sandy Altman Foundation and NIH grant NS14867-11.

REFERENCES

1. Muehllehner G, Karp JS, Mankoff DA, Beerbohm D, Ordonez CE. Design and performance of a new positron tomograph. *IEEE Trans Nucl Sci* 1988; 35:670–674.
2. Kopelson G, Linggood RM. Intramedullary spinal cord astrocytoma versus glioblastoma. The prognostic importance of histologic grade. *Cancer* 1982; 50:732–735.
3. Blasberg RG, Groothuis DR, Molnar P. The application of quantitative autoradiographic measurements in experimental brain tumors. *Semin Neurology* 1981; 1:203–223.
4. DiChiro G. Positron emission tomography using [^{18}F]fluorodeoxyglucose in brain tumors. A powerful diagnostic and prognostic tool. *Invest Radiol* 1987; 22:360–371.
5. Alavi JB, Alavi A, Chawluk J, et al. Positron emission tomography in patients with glioma: a predictor of prognosis. *Cancer* 1988; 62:1074–1078.
6. Francavilla TL, Miletich RS, DiChiro G, Patronas NJ, Rizzoli HV, Wright DC. Positron emission tomography in the detection of malignant degeneration of low-grade gliomas. *Neurosurg* 1989; 24:1–5.
7. Patronas NJ, Brooks RA, DeLaPaz RL, Smith BH, Kornblith PL, DiChiro G. Glycolytic rate (PET) and contrast enhancement (CT) in human cerebral gliomas. *AJNR* 1983; 4:533–535.
8. Patronas NJ, DiChiro G, Brooks RA, et al. [^{18}F]Fluorodeoxyglucose and positron emission tomography in the evaluation of radiation necrosis of the brain. *Radiology* 1982; 144:885–889.
9. DiChiro G, Oldfield E, Wright DC, et al. Cerebral necrosis after radiotherapy and/or intraarterial chemotherapy for brain tumors: PET and neuropathologic studies. *Am J Rad* 1988; 150:189–197.
10. Valk PE, Budinger TF, Levin V, et al. PET of malignant cerebral tumors after interstitial brachytherapy. *J Neurosurg* 1988; 69:830–838.
11. Patronas NJ, DiChiro G, Kufta C, et al. Prediction of survival in glioma patients by means of positron emission tomography. *J Neurosurg* 1985; 62:816–822.
12. DiChiro G, Oldfield E, Bairamian D, et al. Metabolic imaging of the brain stem and spinal cord: studies with positron emission tomography using ^{18}F-2-deoxyglucose in normal and pathological cases. *J Comp Assist Tomogr* 1983; 7:937–945.